# Water and salt transport characteristics in a soil column in the presence of a low-permeable body

Authors: Guo, Yi, Wang, Quanjiu, Liu, Yang, Zhang, Jihong, and Wei, Kai

Source: Canadian Journal of Soil Science, 102(4) : 991-999

Published By: Canadian Science Publishing

URL: https://doi.org/10.1139/cjss-2022-0061

Canadian Journal of Soil Science

Article

# Water and salt transport characteristics in a soil column in the presence of a low-permeable body

**Yi Guo**[a,b], **Quanjiu Wang**[a,b], **Yang Liu**[a,b], **Jihong Zhang**[a,b], **and Kai Wei**[a,b]

[a]State Key Laboratory of Eco-hydraulic in Northwest Arid Region of China, Xi'an University of Technology, Xi'an 710048, China; [b]School of Water Resource and Hydropower, Xi'an University of Technology, Xi'an 710048, China

Corresponding authors: **Quanjiu Wang** (emails: 15503635823@163.com; wquanjiu@163.com)

## Abstract

Soil water infiltration is an important factor affecting surface runoff, soil erosion, and soil solute transmission. Increasing soil infiltration reduces runoff and erosion. The presence of low-permeable body in soil can enhance soil infiltration capacity. However, different depths of low-permeable body have unknown effects on water infiltration and salt transfer. In this work, we evaluated the effects of low-permeable body with varied depths (control (CK), 0, 0.5, 1, and 1.5 cm) on silty loam soil water and salt movement using 15 soil columns (23 cm internal diameter, 50 cm length). Experimental results showed that low-permeable body increased infiltration rate and wetting front migration rate. Infiltration rate and wetting front propulsion rate decreased with the increase of the burial depth. Compared with the CK, when the depth of wetting front reached 20 cm, the infiltration time of 0, 0.5, 1, and 1.5 cm burial depth treatment was shortened by 72.24%, 56.29%, 44.61%, and 31.01%, respectively. Simultaneously, the existence of low-permeable body led to the increase of soil water content and salt content in the same soil layer, which indicated that the low-permeable body enhanced the soil holding capacity and reduced the salt leakage to the deep soil. Furthermore, the Philip's model and the algebraic model were used to describe the infiltration process. Fitting results showed that the sorptivity in the Philip's model increased with burial depth, while the comprehensive shape coefficient in the algebraic model decreased. Therefore, this study provides a reference for the application of low-permeable body in the improving soil infiltration capacity and controlling salt transport.

**Key words:** low-permeable body, infiltration characteristics, soil moisture distribution, salt transport, infiltration model

## Résumé

L'infiltration de l'eau dans le sol est un facteur important qui affecte le ruissellement en surface, l'érosion du sol et le transport des solutés. Quand l'infiltration augmente, le ruissellement et l'érosion s'amenuisent. La présence d'un corps peu perméable dans le sol peut accroître l'infiltration d'eau. Cependant, on ignore quels effets il pourrait avoir sur l'infiltration et le transport des sels selon la profondeur d'enfouissement. Les auteurs ont évalué les effets d'un corps peu perméable situé à diverses profondeurs (témoin (CK), 0, 0,5, 1, 1,5 cm) sur la concentration d'eau dans un loam limoneux et sur le déplacement des sels en recourant à 15 colonnes de sol (23 cm de diamètre interne, 50 cm de longueur). Les résultats de l'expérience montrent que le corps peu perméable augmente le taux d'infiltration et la vitesse de déplacement du front d'humectation. Ces deux paramètres diminuent à mesure que s'accroît la profondeur de l'enfouissement. Comparativement au traitement CK, où le front d'humectation a atteint 20 cm de profondeur, le temps d'infiltration s'est respectivement raccourci de 72,24 %, 56,29 %, 44,61 % et 31,01 % avec une profondeur d'enfouissement de 0, 0,5, 1 et 1,5 cm. Parallèlement, l'existence d'un corps peu perméable a entraîné une hausse de la teneur en eau dans la même couche de sol, signe que ce corps améliore la capacité de rétention du sol et freine la lixiviation des sels vers de plus grandes profondeurs. Les auteurs ont utilisé le modèle de Philip et le modèle algébrique pour décrire le processus d'infiltration. Quand on ajuste les résultats, on constate que, dans le modèle de Philip, la sorptivité augmente avec la profondeur de l'enfouissement alors que dans le modèle algébrique, c'est le coefficient de la forme générale qui diminue. Cette étude servira de point de référence à l'usage d'un corps peu perméable pour améliorer la capacité d'infiltration et contrôler le déplacement des sels. [Traduit par la Rédaction]

**Mots-clés :** corps peu perméable, paramètres d'infiltration, répartition de l'eau dans le sol, transport des sels, modèle d'infiltration

## Introduction

Soil infiltration refers to the process of soil migration and storage after water enters the soil through the surface, which is an important factor affecting surface runoff, soil erosion, and soil solute transport (Hillel 1998; Mao et al. 2008, 2016; Babaei et al. 2018; Sun et al. 2018). Many studies have proved that soil infiltration capacity is closely related to soil erosion, that is, the higher the soil infiltration capacity, the smaller the surface runoff, and the smaller the soil erosion intensity (Cerda 1999; Kaspar et al. 2001; Zhao et al. 2010; Liang et al. 2020). Therefore, studying the characteristics of soil infiltration and evaluating the ability of soil infiltration are of great significance for the prevention and control of soil erosion.

The Loess Plateau (LP) in China is one of the regions worldwide where severe erosions mostly occur (Zhao et al. 2013). The eroded area reaches 234300 $km^2$, comprising 36.25% of the LP area (Ministry of Water Resources 2010). Average annual soil loss is 2000–2500 $t/km^2$/year (Wang et al. 2021). Soil erosion in LP can be mainly attributed to the unique soil conditions and climate environment (Wen and Deng 2020). The main soil type comprising LP is loess, which is easily eroded by water and wind (Chen et al. 2020). Annual rainfall events, mostly of the rainstorm type, are mainly concentrated in July and August (Tang et al. 2018). High-intensity rainfall events typically result in earlier runoff and higher runoff peaks (Ran et al. 2012; Wei et al. 2014; Chen et al. 2018), causing considerable soil and nutrient losses (Peng and Wang 2012; Krasa et al. 2019). Thus, a suitable method for increasing soil infiltration capacity should be developed to slow the generation of surface runoff and further reduce soil and nutrient losses.

At present, the application of soil amendments to improve the infiltration capacity of soil is widely adopted (Lu et al. 2018; Chen et al. 2020; Luo et al. 2020). The common soil amendments mainly include polyacrylamide (PAM), polysaccharide, and biochar. Polyacrylamide is a linear water-soluble polymer with strong viscosity and hydration, which can adsorb, wrap, and bind soil particles. (Bai et al. 2020). Appropriate application of PAM can increase the cohesion between surface soil particles, maintain good soil structure and its stability, and prevent the occurrence of soil crusts, thereby increasing soil infiltration capacity and reducing surface runoff and soil loss (Ao et al. 2016; Amiri et al. 2017; S.Q. Li et al. 2019; Zheng et al. 2020). However, due to the viscosity of the PAM solution, the application of large doses of PAM will also lead to the reduction of soil water infiltration and conductivity, thereby increasing the surface runoff (Sirjacobs et al. 2000; Yu et al. 2003; Lü et al. 2014). In addition, application method, molecular weight, and soil texture also affect the effect of PAM on soil infiltration capacity, which limits the large-scale application of PAM (Lentz 2003; Wang et al. 2011; Dou et al. 2012). Polysaccharide is a natural high molecular polypeptide derivative, which is easily dispersed in water to form a colloid with certain viscosity. Some studies have shown that an appropriate rate of polysaccharides can improve soil aggregate structure, improve soil infiltration performance, and reduce slope erosion (Jiao et al. 2014; Li et al. 2018; Liu et al. 2018; Lu et al. 2018). However, as in the case of PAM application, both the polysaccharide application rate and the soil texture affected the effect of polysaccharide on improving soil infiltration (Li et al. 2018; Lu et al. 2018). In recent years, biochar produced by artificial pyrolysis of biomass has been shown to have the potential to increase soil infiltration capacity as a soil amendment (Yang et al. 2020). Some studies have demonstrated that the addition of biochar across fields can increase soil water-holding capacity (Case et al. 2012; Basso et al. 2013), reduce nutrient loss (Laird et al. 2010; Uzoma et al. 2011), and enhance soil fertility (Vaccari et al. 2011). However, the application of biochar in the Loess Plateau is limited, because storm runoff can easily lead to biochar transmission and loss (Chen et al. 2020). To sum up, there are still some limitations on applying soil amendment to improve soil infiltration capacity in LP.

Recently, Liu et al. (2020) indicated that burying the low-permeable body in the soil can increase the infiltration capacity of the soil, because the soil-water potential difference will be generated inside and outside the low-permeability body during the infiltration process, which will drive the soil water to flow from the high potential energy to the low potential energy, thereby accelerating the infiltration of soil water. Meanwhile, the presence of low-permeable body in the soil also significantly affected the distribution characteristics of soil water content. The difference of soil water content distribution led to the difference of soil salt distribution, because soil water was not only the solvent of salt, but also the carrier of salt movement (X. Li et al. 2019; Xia et al. 2016; Zhao et al. 2019). Liu's study provides an alternative method for improving soil infiltration by setting a low-permeable buried body in the upper soil. However, the effect of low-permeable body with different burial depths on soil water infiltration and salt transport is not clear. Therefore, we conducted one-dimensional water infiltration experiments to analyze the effects of different depths of buried bodies on cumulative infiltration, infiltration rate, wetting fronts, soil moisture distribution, and salt transport in this study.

## Materials and methods

### Materials

The experimental soil was collected from Fuping County (34°41′N, 108°57′E) located in the hinterland of LP. The soil in the 0–20 cm surface layer was collected. The collected soil samples were air-dried naturally, crushed repeatedly, and passed through a 2 mm sieve prior to physicochemical analysis. Soil composition was determined using a laser particle size analyzer (Mastersizer 2000; Malvern Instruments Ltd., United Kingdom). The detailed physical properties of the soil are shown in Table 1.

### Experimental design

The infiltration experiment setup mainly consisted of three parts: a soil column, a water supply bottle, and a low-permeable buried body (Fig. 1). The soil column was a transparent plexiglass cylinder with an inner diameter of 23 cm and a height of 50 cm. The water supply bottle was a Mahler bottle with an inner diameter of 15 cm and a height of 100 cm; it provided a stable infiltration head for the exper-

**Table 1.** Initial physical properties of soil.

| Soil particle distribution | | | | | | | |
|---|---|---|---|---|---|---|---|
| Clay (%) | Silt (%) | Sand (%) | Soil texture class | BD (g/cm$^3$) | $\theta_i$ (cm$^3$/cm$^3$) | $\theta_s$ (cm$^3$/cm$^3$) | $S_i$ (cm$^3$/cm$^3$) |
| 40.5 | 52.2 | 7.3 | Silty loam | 1.4 | 0.019 | 0.469 | 2.76 |

**Note:** BD, bulk density; $\theta_i$, soil initial moisture content; $\theta_s$, saturated volume moisture content; $S_i$, soil initial salt content.

**Fig. 1.** Experimental setup for one-dimension vertical water infiltration.

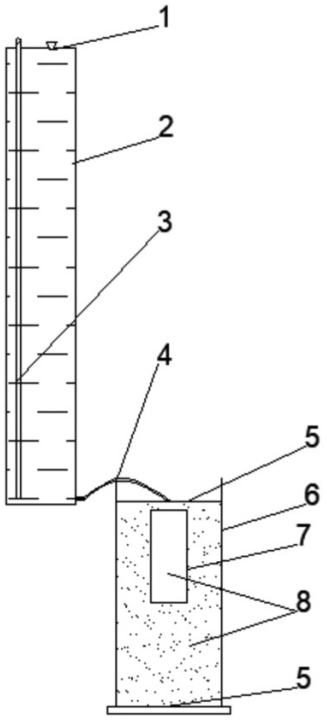


**Fig. 2.** Effect of low-permeable body on cumulative infiltration. [Colour online]

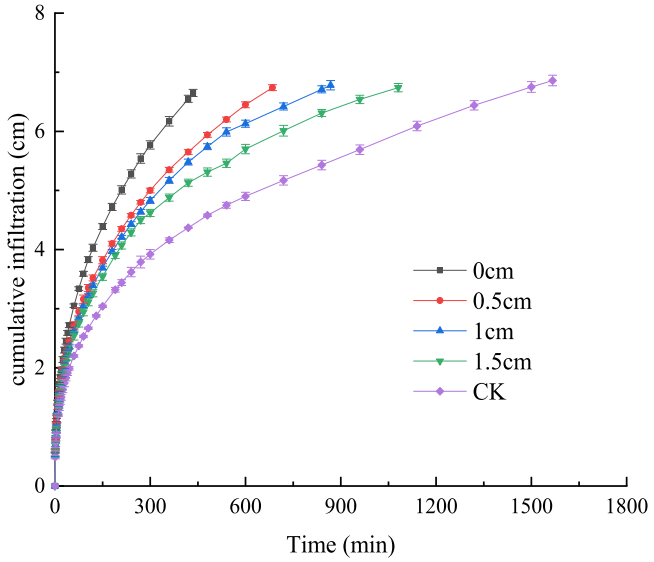


iment. The low-permeable buried body is a cylinder (8 cm internal diameter, 20 cm height) made of polytetrafluoroethylene film that can be filled with soil. Polytetrafluoroethylene film is a kind of polymer material, with numerous micropores on the surface of the film, and the diameters of the micropores are mainly distributed in the range of 0.2−5 μm (Painter 1996). The driving force for moisture migration in small pores between $10^{-7}$ and $10^{-5}$ m is capillary action (Zhao et al. 2015). Five treatments (control treatment (CK), 0, 0.5, 1, and 1.5 cm burial depth of low-permeable) were performed, and three replicates were set up for each treatment, with a total of 15 soil columns. The CK did not include the low-permeable body in the soil column.

The soil filling height of the soil column was set to 40 cm, and it was filled in eight layers (each layer is 5 cm) with a bulk density of 1.40 g/cm$^3$. Control the test water head depth at 2 cm. At the beginning of the experiment, a stopwatch was used to time the time, and the water level of the Martens bottle and the depth of the soil wetting front were recorded regularly according to the principle of density first and then thinning. When the depth of the wetting front reached 20 cm, the water supply was stopped, and at the same time, the surface water was sucked out with a straw, and the soil column was disassembled from the bottom. Put the soil sample into the aluminum box prepared in advance. The soil mass moisture content was determined by the drying method (105 ± 5 °C), and the soil volumetric moisture content was obtained by multiplying the soil bulk density. The dried soil samples were ground and leached according to the soil-water mass ratio of 1:5. After the leaching solution was allowed to stand for eight hours, the conductivity was measured with a DDS-307 conductivity meter, and the soil salinity was obtained.

## Data analysis

In this study, the Philip's infiltration model (Philip 1957) and the Wang's algebraic model (Wang et al. 2003) were used to analyze the characteristics of infiltration under different burying depths. For the vertical infiltration of one-dimensional water in homogeneous soil, the Philip's infiltration model can be simplified as

$$I = St^{\frac{1}{2}} \quad (1)$$

where $I$ is the cumulative infiltration (cm), $S$ is the sorptivity (cm·min$^{-0.5}$), and $t$ is the infiltration time (min).

The algebraic model of one-dimensional vertical water infiltration can not only describe the cumulative infiltration volume well, but also describe the water content distribution at different soil depths after the water infiltration. The algebraic model is as follows:

**Fig. 3.** Effect of low-permeable body on cumulative infiltration. [Colour online]

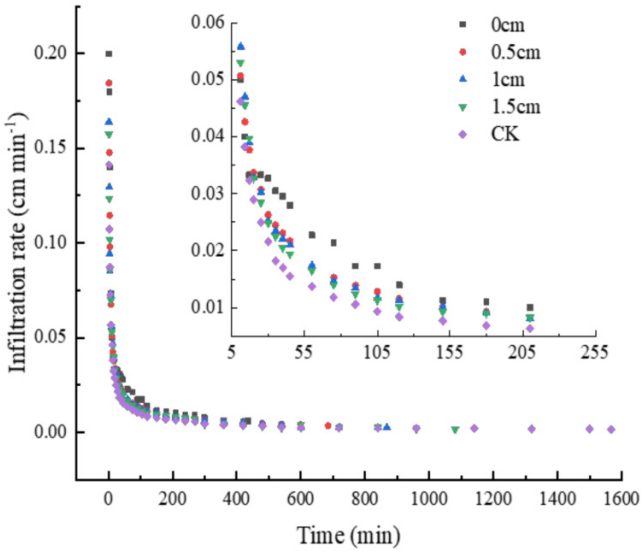


**Fig. 4.** Effect of low-permeable body on wetting front depth. [Colour online]

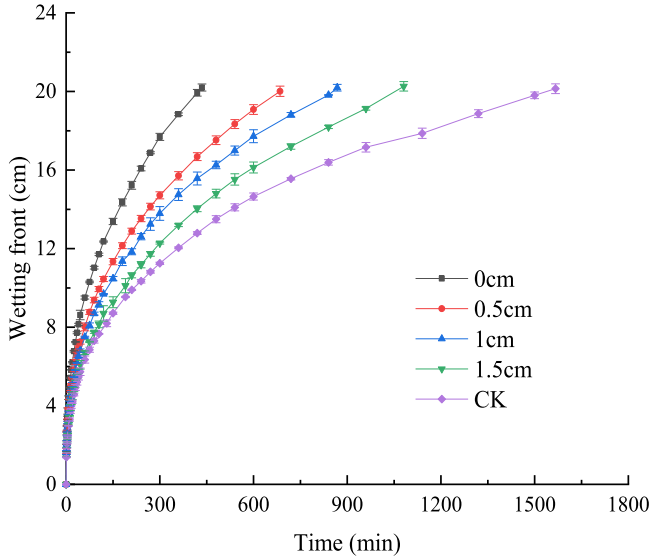


$$(2)\quad I = Z_f\,(\theta_s - \theta_r)\,\frac{1}{1+\alpha}$$

$$(3)\quad \theta = \frac{(\theta_s - \theta_r)}{1+\alpha} Z_f$$

where $Z_f$ is the wetting front depth (cm), $\theta_s$ is the soil saturated water content ($cm^3/cm^3$), $\theta_r$ is the residual soil water content ($cm^3/cm^3$), $\alpha$ is the combined shape coefficient of unsaturated hydraulic conductivity and soil water characteristic curve (dimensionless), and $\theta$ is the soil volume moisture content ($cm^3/cm^3$).

## Results and discussion

### Effect of low-permeable buried body on infiltration characteristics

Figure 2 shows the variation of cumulative infiltration with time under different treatments (CK, 0, 0.5, 1, and 1.5 cm). In general, the cumulative infiltration increased with the increase of infiltration time, and the difference in the cumulative infiltration of different treatments in the early stage of infiltration was not significant. As the experiment continued, the cumulative infiltration between different treatments gradually showed significant differences. Under the same infiltration time, the cumulative infiltration in the treatment with the low-permeable body was greater than that in the CK. After 420 minutes of infiltration, the cumulative infiltration of the 0, 0.5, 1, and 1.5 cm burial depth treatments increased by 49.85%, 29.27%, 25.38%, and 17.40%, respectively, compared with the CK.

Figure 3 shows the variation of infiltration rate under different low-permeable burial depths. At the initial stage of infiltration, the infiltration rate under different treatments varied greatly. Compared with CK, the existence of low-permeable water enhanced the soil infiltration rate. And the infiltration rate decreased with the increase of the burial depth of the low-permeable body. Finally, with the passage of infiltration time, the infiltration rate of each treatment decreased and finally stabilized.

Figure 4 shows the migration of wetting front under different low-permeable burial depths. It can be seen from Fig. 4 that the change of wetting front depth with infiltration time was basically consistent with the cumulative infiltration. The migration rate of wetting front in the treatment with the low-permeable body was higher than that in the CK. After 420 minutes of infiltration, the wetting front of the 0, 0.5, 1, and 1.5 cm burial depth treatments increased by 55.83%, 30.40%, 21.68%, and 9.70%, respectively, compared with the CK. At the end of infiltration (the depth of wetting front is 20 cm), the infiltration time of 0, 0.5, 1, and 1.5 cm burial depth treatment was reduced by 72.24%, 56.29%, 44.61%, and 31.01%, respectively, compared with the CK.

The above results showed that the existence of low-permeable buried body can effectively promote soil infiltration, and the shallower the burial depth was, the more significant the effect was. This was because when the infiltration began, the surface soil water content of the soil column increased rapidly, while the soil water content inside the weakly permeable buried body was relatively low. The soil water potential energy difference between the internal soil and the external soil of the low-permeable buried body forced the soil water to migrate to the low-permeable buried body, thus accelerating the infiltration of soil water and the migration of wetting front. At the same time, it was difficult for a large amount of water to pass through the narrow pores of polytetrafluoroethylene film. Therefore, it could maintain a relatively stable soil water potential difference in the infiltration process and continuously affect the soil water infiltration process. This is consistent with Liu's study (Liu et al. 2020). Moreover, there were obvious differences in infiltration process of different burial depth treatment. This may be

**Fig. 5.** Effect of low-permeable body on soil water content. [Colour online]

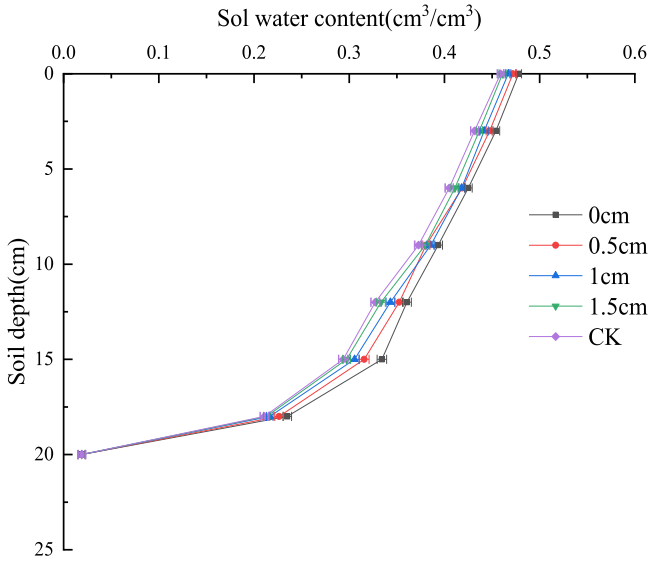


**Fig. 6.** Effect of low-permeable body on soil salt content distribution. [Colour online]

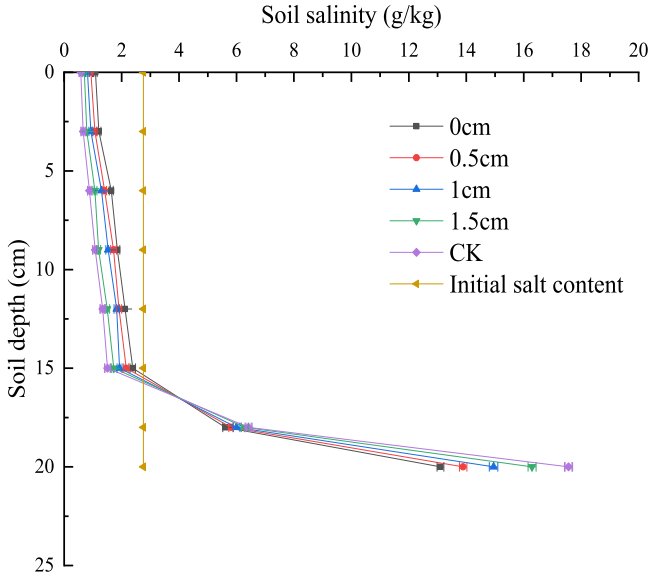


because the shallower the depth of the weakly permeable water body was, the faster the moist soil on the upper layer of the soil column contacted the interface of the buried body, and the soil water potential difference between the soil inside and outside the buried body formed faster, driving the water to migrate from the place with high water content to the place with low water content, resulting in the shallower the burial depth, the greater the soil infiltration capacity.

## Effect of low-permeable buried body on soil water content and soil salt content distribution

The distribution of soil moisture content under different burying depths is presented in Fig. 5. As shown in the figure, the soil volume moisture content under different treatments decreased gradually with an increase in soil depth. The surface soil moisture content was close to the saturated moisture content, and the soil below the wetting front was still the initial moisture content. At the end of the infiltration, the soil moisture content with the low-permeable body was higher than that of the CK. With the increase of the burial depth of the low-permeable body, the soil moisture content gradually decreased. When the burial depth of the low-permeable water body was 0 cm, the soil moisture content was the largest. Compared with the CK, the soil moisture content increased by 4.14%, 5.18%, 4.96%, 5.51%, 10.14%, 13.83%, and 11.42% at 0, 3, 6, 9, 12, 15, and 18 m, respectively. The influence of low-permeable buried body on the distribution of soil water content may be that the low-permeable buried body accelerated the movement of soil water and increased the impulse on soil particles, resulting in the increase of total soil pores, so that more water could be preserved and the soil water content increases.

Figure 6 presents the distribution of soil salt under different burying depths of the buried body. As shown in the figure, soil salt gradually migrated downward with water infiltration and accumulated near the wetting front. The salt content of 0–15 cm soil layer was lower than the initial salt content, and the salt content of 15–20 cm soil layer was higher than the initial salt content. In 0–15 cm soil layer, the soil salt content of low-permeable body was lower than that of the CK, while in 15–20 cm soil layer, the soil salt content of low-permeable buried body was greater than that of the CK. The main reason for this phenomenon was that the infiltration rate of soil water was accelerated, the retention time of water in soil was reduced, and the salt was not fully dissolved in water, which led to the corresponding decrease of salt migration (Wang et al. 2020). The distribution of soil salt content was closely related to soil water transport. When the process of soil infiltration changed, the distribution of soil water content and salt content also showed differences. This is consistent with the previous research results (Li et al. 2008; Ye et al. 2017; Xia et al. 2016; Wei et al. 2021). The effects of different burial depth treatments on soil salt distribution were different. In 0–15 cm soil layer, the soil salt content decreased with the increase of the burial depth of low-permeable body. In 15–20 cm soil layer, the soil salt content increased with the increase of the buried depth of low-permeable body. At a depth of 15 cm, the soil salt content corresponding to the CK and 0, 0.5, 1, and 1.5 cm burial depth treatments were 2.39, 2.16, 1.93, 1.73, and 1.51 g/kg, respectively. Compared with the CK, the four burial depth treatment increased by 25.39%, 20.89%, 14.86%, and 7.23%, respectively. At a depth of 20 cm, the soil salt content corresponding to the CK and the 0, 0.5, 1, and 1.5 cm burial depth treatments were 13.1, 13.89, 14.95, 16.29, and 17.56 g/kg, respectively. Compared with the CK, the four burial depth treatment decreased by 58.27%, 43.05%, 27.81%, and 14.57%, respectively.

Soil erosion is regarded as one of the most serious environmental problems in the world, which directly threatens regional ecological security and sustainable economic and social development (Pimentel and Burgess 2013; Wuepper et al.

**Table 2.** Effect of different burial depths of low-permeable on fitting results of infiltration model.

| Infiltration model | Parameter | Treatment | | | | |
|---|---|---|---|---|---|---|
| | | 0 cm | 0.5 cm | 1 cm | 1.5 cm | CK |
| Philip's model | $S$ (cm min$^{-0.5}$) | 0.3467 | 0.2878 | 0.2646 | 0.2430 | 0.1972 |
| | $R^2$ | 0.9656 | 0.9457 | 0.9370 | 0.9107 | 0.9157 |
| Algebraic model | $\alpha$ | 0.3266 | 0.3417 | 0.3559 | 0.3611 | 0.3732 |
| | $R^2$ | 0.9877 | 0.9995 | 0.9967 | 0.9742 | 0.9973 |

**Fig. 7.** Effect of burial depth of low-permeable body on $S$. [Colour online]

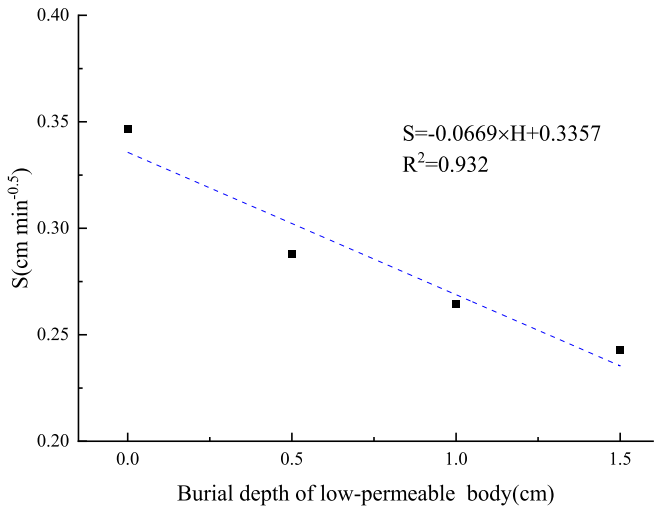


**Fig. 8.** Effect of burial depth of low-permeable body on $\alpha$. [Colour online]

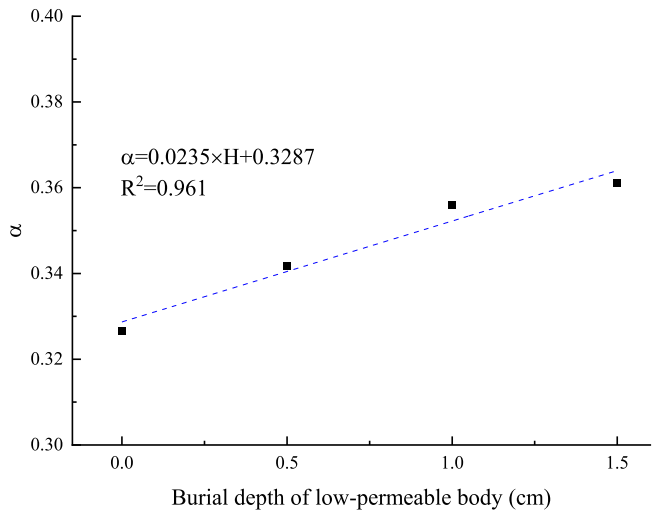


2020). The Loess Plateau is one of the areas with the most serious soil erosion in the world, which has the characteristics of large intensity and wide area (Zhao et al. 2013; Fu et al. 2017; Jin et al. 2021). An important reason for soil erosion in this area is that the rainfall in this area is concentrated, and it is prone to heavy rainstorms. When the rainfall intensity exceeds the soil infiltration capacity, surface runoff will be generated, resulting in erosion of the surface (Wei et al. 2014; Chen et al. 2020). According to previous studies, enhancing the infiltration capacity of soil can ensure that more rainfall infiltrates into the soil, reduce surface runoff and prevent surface erosion (Cerda 1999; Kaspar et al. 2001; Zhao et al. 2010; Liang et al. 2020). In this study, we found that compared with the CK, the presence of a low-permeable body in the soil column led to the increase of soil water content and salt content in the same soil layer, implying that the low-permeable body improves soil holding capacity while reducing salt leakage to the deep soil. Therefore, the low-permeable body has the potential to be applied to the improvement of soil infiltration capacity in the Loess Plateau to reduce runoff and control soil solute transmission.

## Effect of low-permeable buried body on infiltration model parameters

To further analyze and verify the effects of the burying depth of a buried body on soil water infiltration, the measured data were fitted using the Philip's infiltration model (Philip 1957) and the Wang's algebraic infiltration model (Wang et al. 2003), respectively. The obtained $S$ and $\alpha$ values are listed in Table 2. According to Table 2, the average determination coefficients of the two infiltration models were 0.9349 and 0.9911, respectively, indicating that the two infiltration models could well describe the infiltration process of the buried body.

$S$ reflects the ability of soil to absorb or release water by capillary force (Fu et al. 2009; Ning et al. 2019). For the Philip's model, with the increase of the burial depth of the low-permeable body, the value of $S$ decreased gradually, and it was all larger than the CK. The results showed that the low-permeable body could improve soil infiltration capacity, which was consistent with the results of the actual soil water infiltration. The relationship between $S$ and the burying depth was fitted, and the results were presented in Fig. 7, and the determination coefficient was 0.9323. This result indicated a good linear relationship between $S$ and the burying depth. The fitting equation was as follows:

$$S = -0.0669H + 0.3357 \quad (4)$$

where $S$ represents the sorptivity (cm·min$^{-0.5}$), and $H$ represents the burying depth of the buried body (cm).

Figure 8 depicts the variation in the comprehensive shape coefficient $\alpha$ with the burying depth in the algebraic model. As shown in the figure, $\alpha$ increased gradually with an increase in the burying depth. The relationship between the comprehensive shape coefficient $\alpha$ and the burying depth was fitted,

**Fig. 9.** Measured and predicted values of soil moisture content. [Colour online]

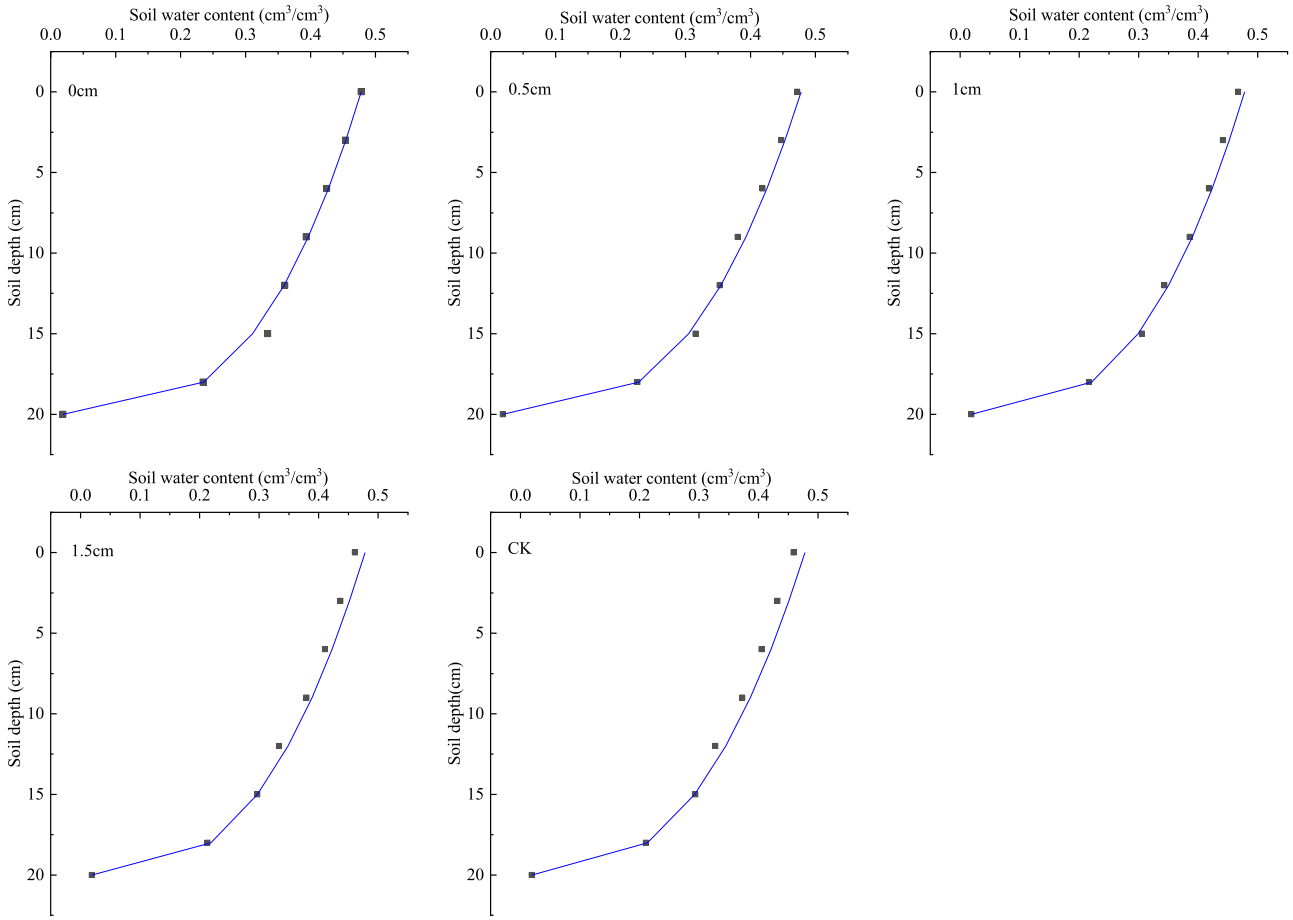


and the fitting determination coefficient was 0.961. The result indicated a good linear relationship between $\alpha$ and the burying depth. The fitting formula was as follows:

$$\alpha = 0.0235H + 0.3287 \quad (5)$$

where $\alpha$ is the combined shape coefficient of the unsaturated hydraulic conductivity and soil water characteristic curve (dimensionless) and $H$ represents the burying depth of the buried body (cm).

## Accuracy analysis of algebraic model describing soil water content after infiltration

The soil moisture content can be calculated by substituting the fitted comprehensive shape coefficient $\alpha$ into (eq. 3) As can be seen from Fig. 9, the calculated value of water content profile was in good agreement with the measured value. To better illustrate the calculation effect of the algebraic model, the error between the calculated value and the measured value of soil moisture content was analyzed. The results showed that the average absolute error of different treatments was no more than 1.48%. It can be seen that the algebraic model could well simulate the soil water content under the condition of low-permeable buried body.

# Conclusions

In this study, the effects of low-permeable buried body under different burying depths on soil infiltration and salt transport were evaluated. We can draw the following conclusions:

(1) Setting low-permeable buried body in soil can improve soil infiltration rate and wetting front propulsion rate. With the increase of the burial depth of the low-permeable body, the infiltration rate and the migration rate of the wetting front continue to decrease.
(2) Compared with the control, the existence of low-permeable body leads to the increase of soil water content and salt content in the same soil layer, which indicates that the low-permeable body enhances the soil holding capacity and reduces the salt leakage to the deep soil. With the increase of the burial depth of the low-permeable body, the soil water content and soil salt content gradually decreased. Compared with the CK, the low-permeable buried body can reduce the migration of soil salt to deep soil relative to that of the control.
(3) The Philip's infiltration model and the Wang's algebraic model were used to describe the process of soil infiltration. The linear relationship between the two parameters and the burying depth of the low-permeable buried body was established. The $S$ in the Philip's infiltration

model increases with the increase of the burial depth of low-permeable body, and the comprehensive shape coefficient $\alpha$ in algebraic infiltration model decreases with the increase of burial depth of low-permeable body.

This study provides a new method to enhance soil infiltration capacity and control soil salt transport. It should be noted that the conclusions of our study were based on silty loam. Soil texture, soil initial water content, and soil bulk density all have great impact on soil infiltration characteristics. Therefore, related research in the above directions should be carried out in the future.

## Acknowledgements

This work was supported by the National Natural Science Foundation of China (41830754 and 52179042), Major Science and Technology projects of the XPCC (2021AA003-2), and Major Science and Technology Projects of Autonomous Region (2020A01003-3)

## Article information

### History dates

Received: 25 April 2022
Accepted: 29 June 2022
Accepted manuscript online: 5 July 2022
Version of record online: 5 October 2022

### Copyright



### Data availability

Data generated or analyzed during this study are provided in full within the published article.

## Author information

### Author ORCIDs

Yi Guo https://orcid.org/0000-0002-2249-5492

### Author contributions

Investigation, data curation, formal analysis, writing (original draft): Y.G.
Conceptualization, writing (review and editing), supervision: Q.W.
Investigation: Y.L., J.Z., K.W.

### Competing interests

The authors declare that they have no competing financial interests or personal relationships that could have appeared to influence the work reported in this paper.

## References

Amiri, E., Emami, H., Mosaddeghi, M.R., and Astaraei, A.R. 2017. Investigating the effect of vetiver and polyacrylamide on runoff, sediment load and cumulative water infiltration. Soil Res. **55**(8): 769–777. doi:10.1071/SR17011.

Ao, C., Yang, P.L., Ren, S.M., Xing, W.M., Li, X., and Feng, X.W. 2016. Efficacy of granular polyacrylamide on runoff, erosion and nitrogen loss at loess slope under rainfall simulation. Environ. Earth Sci. **75**(6): 1–10. doi:10.1007/s12665-015-5110-3.

Babaei, F., Zolfaghari, A.A., Yazdani, M.R., and Sadeghipour, A. 2018. Spatial analysis of infiltration in agricultural lands in arid areas of Iran. Catena, **170**: 25–35. doi:10.1016/j.catena.2018.05.039.

Bai, G.S., Luo, D., Miao, Q.F., Zhou, N., and Du, S.N. 2020. Effects of spraying amounts and application methods of polyacrylamide (PAM) on aeolian sandy soil wind erosion. Trans. Chin. Soc. Agric. Eng. (Trans. CSAE), **36**(10): 90–98. (in Chinese with English abstract)

Basso, A.S., Miguez, F.E., Laird, D.A., Horton, R., and Westgate, M. 2013. Assessing potential of biochar for increasing water-holding capacity of sandy soils. GCB Bioenergy, **5**(2): 132–143. doi:10.1111/gcbb.12026.

Case, S.D.C., McNamara, N.P., Reay, D.S., and Whitaker, J. 2012. The effect of biochar addition on $N_2O$ and $CO_2$ emissions from a sandy loam soil-The role of soil aeration. Soil Biol. Biochem. **51**: 125–134. doi:10.1016/j.soilbio.2012.03.017.

Cerda, A. 1999. Parent material and vegetation affect soil erosion in eastern Spain. Soil Sci. Soc. Am. J. **63**(2): 362–368. doi:10.2136/sssaj1999.03615995006300020014x.

Chen, H., Zhang, X.P., Abla, M., Lü, D., Yan, R., Ren, Q.F., and Yang, X.H. 2018. Effects of vegetation and rainfall types on surface runoff and soil erosion on steep slopes on the Loess Plateau, China. Catena, **170**: 141–149. doi:10.1016/j.catena.2018.06.006.

Chen, X.P., Zhou, B.B., Wang, Q.J., Tao, W.H., and Lin, H. 2020. Nanobiochar reduced soil erosion and nitrate loss in sloping fields on the Loess Plateau of China. Catena, **187**: 104346. doi:10.1016/j.catena.2019.104346.

Dou, C.Y., Li, F.H., and Wu, L.S. 2012. Soil erosion as affected by polyacrylamide application under simulated furrow irrigation with saline water. Pedosphere, **22**(5): 681–688. doi:10.1016/S1002-0160(12)60053-8.

Fu, B., Wang, S., Liu, Y., Liu, J., Liang, W., and Miao, C. 2017. Hydrogeomorphic ecosystem responses to natural and anthropogenic changes in the Loess Plateau of China. Annu. Rev. Earth Planet. Sci. **45**: 223–243. doi:10.1146/annurev-earth-063016-020552.

Fu, Q.P., Wang, Q.J., and Fan, J. 2009. Study on the time scales of soil sorptivety determined by Philip equation. Agric. Res. Arid Areas, **27**(4): 65–70. (in Chinese with English abstract)

Hillel, D. 1998. Environmental Soil Physics. Academic Press, New York.

Jiao, N., Wang, Z.L., and Liu, J.E. 2014. Regulating effect of Jag C162 application on infiltration on loess slope. Bull. Soil Water Conserv. **34**(1): 25–30. (in Chinese with English abstract)

Jin, F., Yang, W., Fu, J., and Li, Z. 2021. Effects of vegetation and climate on the changes of soil erosion in the Loess Plateau of China. Sci. Total Environ. **773**: 145514. doi:10.1016/j.scitotenv.2021.145514. PMID: 33588223.

Kaspar, T.C., Radke, J.K., and Laflen, J.M. 2001. Small grain cover crops and wheel traffic effects on infiltration, runoff, and erosion. J. Soil Water Conserv. **56**(2): 160–164.

Krasa, J., Dostal, T., Barbora, J., Bauer, M., and Devaty, J. 2019. Soil erosion as a source of sediment and phosphorus in rivers and reservoirs—watershed analyses using WaTEM/SEDEM. Environ. Res. **171**: 470–483. doi:10.1016/j.envres.2019.01.044. PMID: 30739021.

Laird, D., Fleming, P., Wang, B., Horton, R., and Karlen, D. 2010. Biochar impact on nutrient leaching from a Midwestern agricultural soil. Geoderma, **158**(3-4): 436–442. doi:10.1016/j.geoderma.2010.05.012.

Lentz, R.D. 2003. Inhibiting water infiltration with polyacrylamide and surfactants: applications for irrigated agriculture. J. Soil Water Conserv. **58**(5): 290–300.

Li, S.Q., Xu, H.L., and Ao, C. 2019. Polyacrylamide and rill flow rate effects on erosion and ammonium nitrogen losses. Water Air Soil Pollut. **230**(1): 1–14.

Li, X., Xia, J., Zhao, X., and Chen, Y. 2019. Effects of planting Tamarix chinensis on shallow soil water and salt content under different groundwater depths in the Yellow River Delta. Geoderma, **335**: 104–111. doi:10.1016/j.geoderma.2018.08.017.

Li, Y.Y., Wang, Z.L., Wu, B., Liu, J.E., and Jiao, N. 2018. Impacts of natural polymer derivative neutral polysaccharide Jag S and cationic hydroxypropyl polysaccharide Jag C162 on rainfall infiltration on an experimental loess hillslope. Soil Sci. Plant Nutr. **64**(2): 244–252.

Li, Z., Liu, X., Zhang, X., and Li, W. 2008. Infiltration of melting saline ice water in soil columns: consequences on soil moisture and salt content. Agric. Water Manage. **95**(4): 498–502. doi:10.1016/j.agwat.2007.12.001.

Liang, Y., Jiao, J.Y., Tang, B.Z., Cao, B.T., and Li, H. 2020. Response of runoff and soil erosion to erosive rainstorm events and vegetation restoration on abandoned slope farmland in the Loess Plateau region, China. J. Hydrol. **584**: 124694.

Liu, J.E., Wang, Z.L., and Li, Y.Y. 2018. Efficacy of natural polymer derivatives on soil physical properties and erosion on an experimental loess hillslope. Int. J. Environ. Res. Public Health, **15**(1): 1–14.

Liu, Y., Wang, Q.J., Gou, L.N., Zhang, J.H., and Wei, K. 2020. Effect of air-permeable and water-proof buried body on soil water infiltration and solute transport. J. Soil Water Conserv. **34**(4): 152–157. (in Chinese with English abstract).

Lu, S.J., Wang, Z.L., Hu, Y.X., Liu, B.Y., and Liu, J.E. 2018. Effectiveness and durability of polyacrylamide (PAM) and polysaccharide (Jag C 162) in reducing soil erosion under simulated rainfalls. Water, **10**(3): 257. doi:10.3390/w10030257.

Lü, W., Li, S., Lei, T., and Li, F. 2014. Effects of polyacrylamide application on rainfall runoff in composite slopes of loessial soil. Trans. Chin. Soc. Agric. Eng. **30**(6): 71–79. (in Chinese with English abstract)

Luo, C.Y., Yang, J.J., Chen, W., and Han, F. 2020. Effect of biochar on soil properties on the Loess Plateau: results from field experiments. Geoderma, **369**: 114323. doi:10.1016/j.geoderma.2020.114323.

Mao, L.L., Braits, V.F., Pan, Y.H., Liu, H., and Lei, T.W. 2008. Methods for measuring soil infiltration: state of the art. Int. J. Agric. Biol. Eng. **1**(1): 22–30.

Mao, L.L., Li, Y.Z., Hao, W.P., Zhou, X.N., Xu, C.Y., and Lei, T.W. 2016. A new method to estimate soil water infiltration based on a modified Green–Ampt model. Soil Tillage Res. **161**: 31–37. doi:10.1016/j.still.2016.03.003.

Ministry of Water Resources. P.R. China. 2010. Chinese Academy of Sciences & Chinese Academy of Engineering. Control soil and water loss and ecological security in China: policy of soil and water loss. Science Press , Beijing.

Ning, S.R., Jumai, H., Wang, Q.J., Zhou, B.B., Su, L.J., Shan, Y.Y., and Zhang, J.H. 2019. Comparison of the effects of polyacrylamide and sodium carboxymethylcellulose application on soil water infiltration in sandy loam soils. Adv. Polym. Technol. 1–7. doi:10.1155/2019/6869454

Painter, C.J. 1996. Waterproof, breathable fabric laminates: a perspective from film to market place. J. Coated Fabrics, **26**(2): 107–130. doi:10.1177/152808379602600202.

Peng, T., and Wang, S.J. 2012. Effects of land use, land cover and rainfall regimes on the surface runoff and soil loss on karst slopes in southwest China. Catena, **90**: 53–62. doi:10.1016/j.catena.2011.11.001.

Philip, J.R. 1957. Theory of infiltration: 1. The infiltration equation and its solution. Soil Sci. **83**: 345–358. doi:10.1097/00010694-195705000-00002.

Pimentel, D., and Burgess, M. 2013. Soil erosion threatens food production. Agriculture, **3**(3): 443–463. doi:10.3390/agriculture3030443.

Ran, Q.H., Su, D.Y., Li, P., and He, Z.G. 2012. Experimental study of the impact of rainfall characteristics on runoff generation and soil erosion. J. Hydrol. **424**: 99–111. doi:10.1016/j.jhydrol.2011.12.035.

Sirjacobs, D., Shainberg, I., Rapp, I, and Levy, G.J. 2000. Polyacrylamide, sediments, and interrupted flow effects on rill erosion and intake rate. Soil Sci. Soc. Am. J. **64**(4): 1487–1495. doi:10.2136/sssaj2000.6441487x.

Sun, D., Yang, H., Guan, D.X., Yang, M., Wu, J.B. Yuan, F.H., et al. 2018. The effects of land use change on soil infiltration capacity in China: a meta-analysis. Sci. Total Environ. **626**: 1394–1401. doi:10.1016/j.scitotenv.2018.01.104. PMID: 29898546.

Tang, X., Miao, C.y., Xi, Y., Duan, Q.Y., Lei, X.H., and Li, H. 2018. Analysis of precipitation characteristics on the loess plateau between 1965 and 2014, based on high-density gauge observations. Atmos. Res. **213**: 264–274. doi:10.1016/j.atmosres.2018.06.013.

Uzoma, K.C., Inoue, M., Andry, H., Zahoor, A., and Nishihara, E. 2011. Influence of biochar application on sandy soil hydraulic properties and nutrient retention. J. Food, Agric. Environ. **9**(3–4): 1137–1143.

Vaccari, F.P., Baronti, S., Lugato, E., Genesio, L., Castaldi, S., Fornasier, F., and Miglietta, F. 2011. Biochar as a strategy to sequester carbon and increase yield in durum wheat. Eur. J. Agron. **34**(4): 231–238. doi:10.1016/j.eja.2011.01.006.

Wang, A.I., Li, H.F., and Yang, S.M. 2011. Effect of polyacrylamide application on runoff, erosion, and soil nutrient loss under simulated rainfall. Pedosphere, **21**(5): 628–638. doi:10.1016/S1002-0160(11)60165-3.

Wang, Q.J., Horton, R., and Shao, M.A. 2003. Algebraic model for one-dimensional infiltration and soil water distribution. Soil Sci. **168**(10): 671–676. doi:10.1097/01.ss.0000095140.68539.8e.

Wang, Q.J., Xie, J.B., Zhang, J.H., Wei, K., Sun, Y., and Li, Z.Y. 2020. Effects of magnetic filed strength on magnetized water infiltration and soil water and salt movement. Trans. Chin. Soc. Agric. Eng. **051**(002): 292–298. (in Chinese with English abstract)

Wang, X.Q., Wang, Z.S., Xiao, J., He, M.Y., Zhang, F., Pan, Y.H., and Jin, Z.D. 2021. Soil erosion fluxes on the central Chinese Loess Plateau during CE 1811 to 1996 and the roles of monsoon storms and human activities. Catena, **200**: 105148. doi:10.1016/j.catena.2021.105148.

Wei, K., Zhang, J., Wang, Q., Chen, Y., and Ding, Q. 2021. Effects of ionized brackish water and polyacrylamide application on infiltration characteristics and improving water retention and reducing soil salinity. Can. J. Soil Sci. **101**(2): 324–334. doi:10.1139/cjss-2020-0099.

Wei, W., Jia, F.Y., Yang, L., Chen, L.D., Zhang, H.D., and Yu, Y. 2014. Effects of surficial condition and rainfall intensity on runoff in a loess hilly area, China. J. Hydrol. **513**: 115–126. doi:10.1016/j.jhydrol.2014.03.022.

Wen, X., and Deng, X.Z. 2020. Current soil erosion assessment in the Loess Plateau of China: a minireview. J. Cleaner Prod. **276**: 1–10. doi:10.1016/j.jclepro.2020.123091.

Wuepper, D., Borrelli, P., and Finger, R. 2020. Countries and the global rate of soil erosion. Nat. Sustain. **3**(1): 51–55. doi:10.1038/s41893-019-0438-4.

Xia, J., Zhang, S., Zhao, X., Liu, J., and Chen, Y. 2016. Effects of different groundwater depths on the distribution characteristics of soil-Tamarix water contents and salinity under saline mineralization conditions. Catena, **142**: 166–176. doi:10.1016/j.catena.2016.03.005.

Yang, Z., Sun, T.R., Subdiaga, E., Obst, M., Haderlein, S.B., Maisch, M., and Kappler, A. 2020. Aggregation-dependent electron transfer via redox-active biochar particles stimulate microbial ferrihydrite reduction. Sci. Total Environ. **703**: 135515. doi:10.1016/j.scitotenv.2019.135515. PMID: 31761354.

Ye, X., Huang, Z., Fan, Y., Wang, Z., Xia, Z., and Liu, Z. 2017. Dynamics of soil moisture and salt content after infiltration of saline ice meltwater in saline-sodic soil columns. Pedosphere, **27**(6): 1116–1124.

Yu, J., Lei, T., Shainberg, I., Mamedov, A.I., and Levy, G.J. 2003. Infiltration and erosion in soils treated with dry PAM and gypsum. Soil Sci. Soc. Am. J. **67**(2): 630–636. doi:10.2136/sssaj2003.6300.

Zhao, G., Mu, X., Wen, Z., Wang, F., and Gao, P. 2013. Soil erosion, conservation, and eco-environment changes in the Loess Plateau of China. Land Degradation. Develop. **24**(5): 499–510.

Zhao, X., Xia, J., Chen, W., Chen, Y., Fang, Y., and Qu, F. 2019. Transport characteristics of salt ions in soil columns planted with Tamarix chinensis under different groundwater levels. PLoS ONE, **14**(4): 1–17. doi:10.1371/journal.pone.0215138.

Zhao, Y.Y., Wang, Y.J., Wang, Y.Q., Zhao, Z.J., Wu, Y., and Chen, L. 2010. Effects of structures of plantation forests on soil infiltration characteristics in source water protect areas in northern Chongqing City. Acta Ecol. Sin. **30**(15): 4162–4172. (in Chinese with English abstract)

Zhao, Z. 2015. Simulation and experimental research on drying of grain packing porous media. Shaanxi University of Science & Technology,Xi'an, China.

Zheng, M., Huang, Z., Ji, H.D., Qiu, F.G., Zhao, D.Y., Bredar, A.R., and Farnum, B.H. 2020. Simultaneous control of soil erosion and arsenic leaching at disturbed land using polyacrylamide modified magnetite nanoparticles. Sci. Total Environ. **702**: 134997. doi:10.1016/j.scitotenv.2019.134997. PMID: 31726340.